THE EFFECT OF FUEL VARIATION ON FLAME PROPAGATION IN IC ENGINES WITH STRONG MACRO FLOWS

Zoran Jovanovic, Zoran Masonicic, Zlatomir Živanovic, Milan Milovanovic

Institute of Nuclear Sciences "VINČA", University of Belgrade, Serbia, E-mail: zoranj@vin.bg.ac.rs

Abstract: *In this paper some results concerning the evolution of flame propagation through unburnt mixture of two different hydrocarbon fuels,such as CH4 and C8H18, in engines with strong macro flows were presented. Flame propagation was represented by the evolution of spatial distribution of temperature in various cutplanes within combustion chamber. Flame front location was determined in zones with maximum temperature gradient. All results were obtained by dint of multidimensional modeling of reactive flows in arbitrary geometry of IC engine combustion chamber with moving boundaries. In 4.-valve engines the fluid flow pattern during intake is characterized with organized tumble motion pursued by small but clearly legible deterioration in the vicinity of BDC. During compression the fluid flow pattern is entirely three-dimensional and fully controlled by vortex motion located in the central part of the chamber. For that reason these engines are designated as IC engines with strong macro flows (swirl, squish, tumble) yielding non-spherical flame shapes usually encountered in quiescent flows. Flame propagation results for both fuels were obtained with eddy-viscosity model i.e. with standard k-ε model of turbulence. The interplay between fluid flow pattern and flame propagation is entirely invariant as regards fuel variationindicating that flame propagation through unburnet mixture of CH4 and C8H18 hydrocarbon fuels is not chemically controlled but controlled by dint of turbulent diffusion.*

KEYWORDS*: FLAME PROPAGATION, TURBULENCE*

1. Introduction

It is known for a long time that various types of organized flows in combustion chamber of IC engines are of predominant importance for combustion particularly with regards to flame front shape and its propagation. Some results related to the isolated or synergic effect of squish and swirl on flame propagation in various combustion chamber layouts are already analyzed and published [1, 2] but results concerning the isolated or combined effect of the third type of organized flow i.e. tumble are relatively less presented and sometimes ambiguous [3, 4]. For instance some authors [5] studied the development of swirl and tumble in five different intake valve configurations and found that when both inlet valves are opened no defined tumble flow structure was created rendering quick vortices dissipation before BDC. In spite of the fact that tumble flow is inherent to multi-valve engines some authors have demonstrated that some two-valve engines exhibit characteristics similar to tumble flow [6, 7]. In addition, the fairly similar fluid flow patterns in the vicinity of BDC in various combustion chamber geometries yield entirely different fluid flow patterns, spatial distribution of kinetic energy of turbulence and integral length scales of turbulence in the vicinity of TDC [8]. In such occasions the significance of organized tumble flow is fairly relative. Some theoretical and experimental results show that tumble is of prime importance for specific power and fuel economy increase in modern engines with multi-valve systems.

From the theory of turbulence is known that vortex filament subjected to compression reduces its length and promotes rotation around its axis yielding the movement on the larger scale ("spin-up" effect).

It can be presumed that tumble pursues the same rule i.e. the destruction of formed and expressive tumble during compression stroke generates the higher turbulence intensity and larger integral length scale of turbulence in the vicinity of TDC contributing to the flame kernel formation period reduction and faster flame propagation thereafter. The aforementioned logic imposes the conclusion that the most beneficial fluid flow pattern in the vicinity of BDC is well shaped high intensity tumble. Some additional objectives in this paper were qualitative and quantitative characterization of fluid flow pattern during induction and compression in a particular 4-valve engine, the analysis of the valve/port assembly from the point of compliance with presumed ideal fluid flow pattern and the clout of turbulence model variation on fluid flow and turbulence parameters.

2. Model and computational method

The analysis of this type is inherent to multidimensional numerical modeling of non-reactive fluid flow and therefore it is quite logical to apply such a technique particularly due to fact that it is the only technique that encompasses the valve/port geometry layout in an explicit manner. In lieu of the fact that, in its essence, multidimensional models require initial and boundary conditions only their applications is fairly complicated and imply some assumptions and simplifications [9]. The full 3D conservation integral form of unsteady equations governing turbulent motion of non-reactive mixture of ideal gas is solved on fine computational grid with moving boundaries (piston and valves) in physical domain (500.000-980.000 cells) by dint of AVL FIRE code [10]. In this case the numerical solution method is based on a fully conservative finite volume approach. All dependent variables such as momentum, pressure, density, turbulence kinetic energy, dissipation rate, and passive scalar are evaluated at the cell center. A second-order midpoint rule is used for integral approximation and a second order linear approximation for any value at the cell-face. A diffusion term is incorporated into the surface integral source after employment of the special interpolation practice. The convection is solved by a variety of differencing schemes (upwind or donor cell, interpolated donor cell, quasi second order differencing, central differencing, MINMOD and SMART). The rate of change is differenced by using implicit schemes i.e. Euler implicit scheme and three time level implicit scheme of second order accuracy. The overall solution procedure is iterative and is based on the Semi-Implicit Method for Pressure-Linked Equations algorithm (SIMPLE). For the solution of a linear system of equations, a conjugate gradient type of solver (CGS) is used. In this quest a nearly forty years old k-ε model of turbulence was used. This model based on Boussinesq's assumption is certainly the most widely used model of turbulence for engineering computations. On the contrary to some other models, such as Reynolds-stress closure model [11], its implementation is numerically robust due to simplicity of the model and at the same provides an acceptable level of accuracy for particular applications.

The second one, relatively recent k-ξ-f model of turbulence i.e. eddy-viscosity model based on Durbin's elliptic relaxation concept [13, 14] and its effect on flame propagation was already analyzed [12] and is not under the scope of this paper. This model solves a transport equation for the velocity scale ratio ξ instead of imaginary turbulent normal stress component. In addition, the pertinent hybrid boundary conditions are prerequisite.

3. Results and discussion

The flame propagation through unburnt mixture of two different hydrocarbon fuels, such as CH4 and C8H18, was analyzed by dint of the evolution of spatial distribution of temperature, represented in form of iso-contours, in six cutplanes passing through various parts of fairly complicated IC engine combustion chamber geometry layout presented in figures 1 and 2. Obviously, combustion chamber is constrained with dual intake and exhaust valves. The basic block

data sheet consists of bore/stroke ratio = 80/81.4 mm, squish gap=1.19 mm, engine speed RPM = 5500 min^{-1} and mixture quality λ=1. It should be stated that maximum valve lift is 6.95 mm for intake valves and 6.63 mm for exhaust valves while the other geometrical data (relative location, valve shape etc.) could be seen in fig.1 and 2.

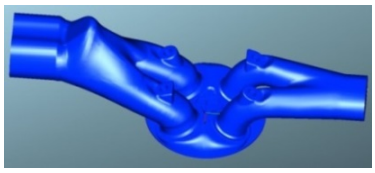

***Figure.1**. Perspective view of the combustion chamber geometry layout with 4-valves (upper view)*

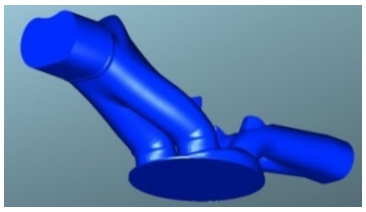

***Figure.2**. Perspective view of the combustion chamber geometry layout with 4-valves (bottom view)*

The first cutplane is x-z plane passing simultaneously through both one intake and one exhaust valve displaced 1.16cm along y axe far away from the symmetry plane (y=const.=1.16). The second cutplane is x-z symmetry plane itself (y=const.=0). The third and fourth cutplanes are y-z planes passing either through both intake or exhaust valves respectively and displaced appropriately forward and backward along x axe (x= ± const.).The fifth cutplane is x-y plane passing through mid-height of the combustion chamber while the sixth cutplane is x-y plane passing through squish zone.

The flame propagation i.e. the evolution of spatial distribution of temperature in the first cutplane for C8H18 and CH4 fuels is shown in figs. 3-10.

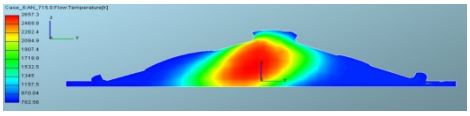

***Figure 3**. Spatial distribution of temperature in x-z plane, y=const. (1.16) at 355 deg. ATDC, k-ε, C8H18*

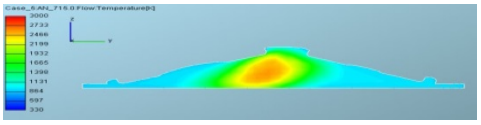

***Figure 4**. Spatial distribution of temperature in x-z plane, y=const. (1.16) at 355 deg. ATDC, k-ε, CH4*

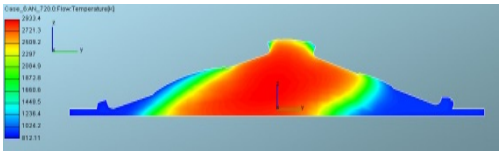

***Figure 5**. Spatial distribution of temperature in x-z plane, y=const. (1.16) at 360 deg. ATDC, k-ε, C8H18*

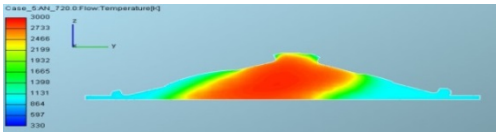

***Figure 6**. Spatial distribution of temperature in x-z plane, y=const. (1.16) at 360 deg. ATDC, k-ε, CH4*

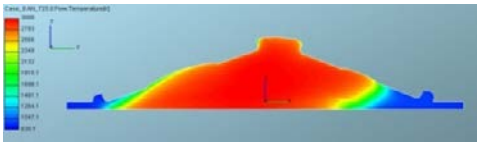

***Figure 7**. Spatial distribution of temperature in x-z plane, y=const. (1.16) at 365 deg. ATDC, k-ε, C8H18*

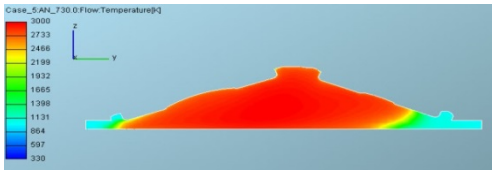

***Figure 8**. Spatial distribution of temperature in x-z plane, y=const. (1.16) at 365 deg. ATDC, k-ε, CH4*

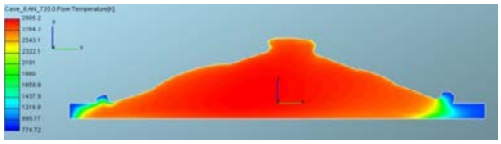

***Figure 9**. Spatial distribution of temperature in x-z plane, y=const. (1.16) at 370 deg. ATDC, k-ε, C8H18*

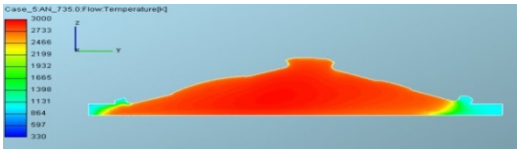

***Figure 10**. Spatial distribution of temperature in x-z plane, y=const. (1.16) at 370 deg. ATDC, k-ε, CH4*

The flame propagation i.e. the evolution of spatial distribution of temperature in the second symmetry cutplane for C8H18 and CH4 fuels is shown in figs. 11-20.

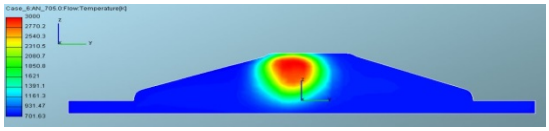

***Figure 11**. Spatial distribution of temperature in x-z symmetry plane, y=0.0 at 345 deg. ATDC, k-ε, C8H18*

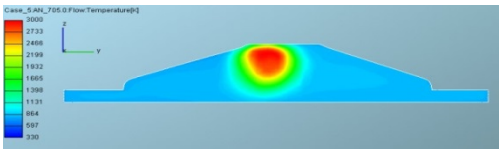

***Figure 12**. Spatial distribution of temperature in x-z symmetry plane, y=0.0 at 345 deg. ATDC, k-ε, CH4*

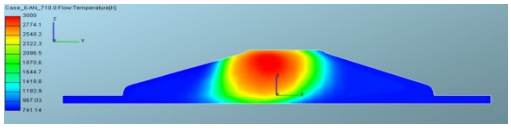

***Figure 13**. Spatial distribution of temperature in x-z symmetry plane, y=0.0 at 350 deg. ATDC, k-ε, C8H18*

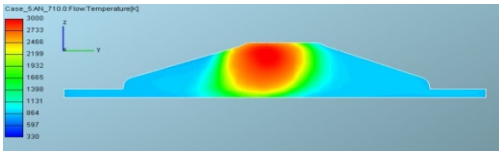

***Figure 14**. Spatial distribution of temperature in x-z symmetry plane, y=0.0 at 350 deg. ATDC, k-ε, CH4*

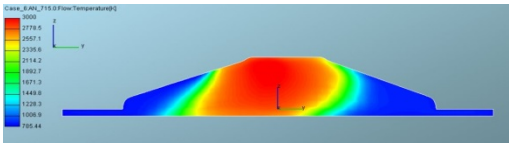

***Figure 15**. Spatial distribution of temperature in x-z symmetry plane, y=0.0 at 355 deg. ATDC, k-ε, C8H18*

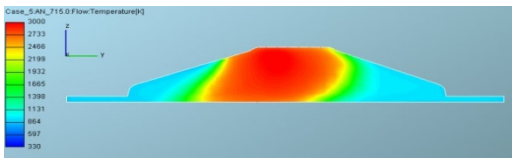

***Figure 16**. Spatial distribution of temperature in x-z symmetry plane, y=0.0 at 355 deg. ATDC, k-ε, CH4*

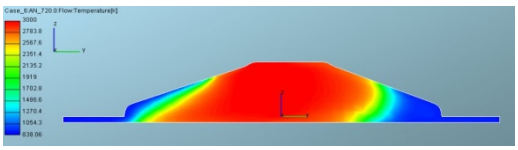

***Figure 17**. Spatial distribution of temperature in x-z symmetry plane, y=0.0 at 360 deg. ATDC, k-ε, C8H18*

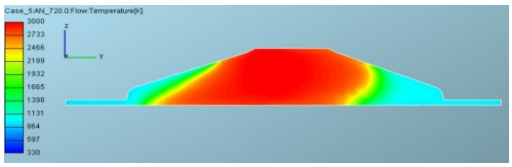

***Figure 18**. Spatial distribution of temperature in x-z symmetry plane, y=0.0 at 360 deg. ATDC, k-ε, CH4*

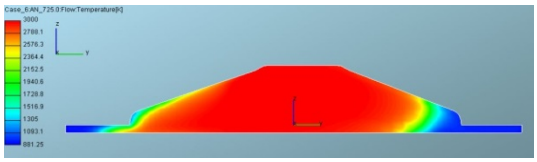

***Figure 19**. Spatial distribution of temperature in x-z symmetry plane, y=0.0 at 365 deg. ATDC, k-ε, C8H18*

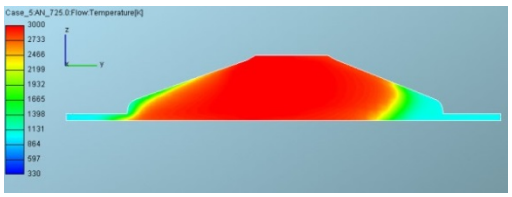

***Figure 20**. Spatial distribution of temperature in x-z symmetry plane, y=0.0 at 365 deg. ATDC, k-ε, CH4*

The flame propagation i.e. the evolution of spatial distribution of temperature in the sixth cutplane for C8H18 and CH4 fuels is shown in figs. 21-30.

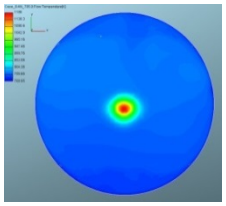

***Figure 21**. Spatial distribution of temperature in x-y plane passing through squish zone at 345 deg. ATDC, k-ε, C8H18*

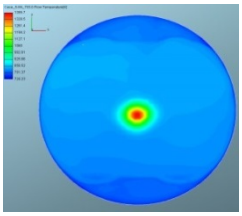

***Figure 22**. Spatial distribution of temperature in x-y plane passing through squish zone at 345 deg. ATDC, k-ε, CH4*

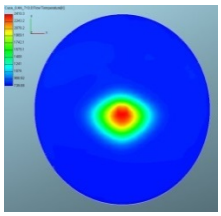

***Figure 23**. Spatial distribution of temperature in x-y plane passing through squish zone at 350 deg. ATDC, k-ε, C8H18*

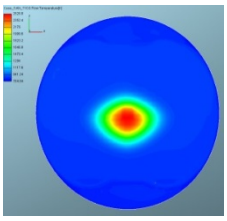

***Figure 24**. Spatial distribution of temperature in x-y plane passing through squish zone at 350 deg. ATDC, k-ε, CH4*

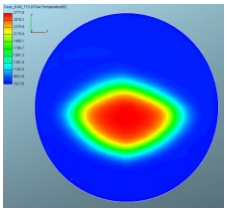

***Figure 25**. Spatial distribution of temperature in x-y plane passing through squish zone at 355 deg. ATDC, k-ε, C8H18*

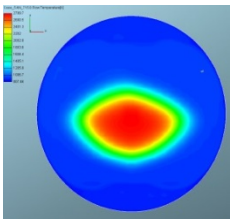

***Figure 26**. Spatial distribution of temperature in x-y plane passing through squish zone at 355 deg. ATDC, k-ε, CH4*

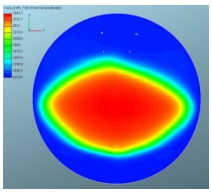

***Figure 27**. Spatial distribution of temperature in x-y plane passing through squish zone at 360 deg. ATDC, k-ε, C8H18*

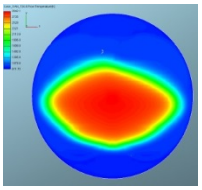

***Figure 28**. Spatial distribution of temperature in x-y plane passing through squish zone at 360 deg. ATDC, k-ε, CH4*

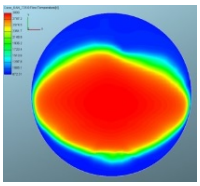

***Figure 29**. Spatial distribution of temperature in x-y plane passing through squish zone at 365 deg. ATDC, k-ε, C8H18*

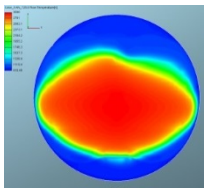

***Figure 30**. Spatial distribution of temperature in x-y plane passing through squish zone at 365 deg. ATDC, k-ε, CH4*

Obviously neither differences in flame propagation nor in flame front shape in all cutplanes were encountered for both hydrocarbon fuels used (C8H18 and CH4) yielding the conclusion that flame front shape and its displacement are not chemically controlled but controlled by dint of turbulent diffusion i.e. by high intensity of turbulence and cascade process of tearing or breaking up large vortices into smaller ones and their dissipation into heat.

Anyhow, at least five conflicting mechanisms, acting in concert, are of prime importance for the determination of flame front shape and its displacement. These are, *inter alia*, flame generated turbulence, compression by the flame, increase of the viscosity behind the flame front, the sign and the magnitude of the density gradient across the flame front and the effect of large heat release due to chemical reactions.

Namely flame propagation through un-burnt mixture causes the acceleration of the hot gas in front of the flame front. In the case of shear the production of turbulence increases with the effect of flame acceleration thereafter. In the compressed zone in front of the flame front the divergence of the mean velocity is negative yielding the generation of turbulence as well. In addition the sign and the magnitude of the density gradient within the flame affect the diffusion of turbulence. Referring to the energy conservation equation one can find the maximum enthalpy in the zone of minimal density i.e. behind the flame front so these higher temperatures cause the intensive increase of viscosity with the consequential increase of Re_t-number, the increase of viscous dissipation of turbulence and shifting of the velocity fluctuations to the low frequency part of spectrum. In the heat release zone the dilatation of turbulence reduces the turbulent kinetic energy yielding attenuation of the fluid flow.

4. Conclusions

The flame front shape and its displacement in IC engine combustion chamber with strong macro flows are entirely invariant as regards fuel variation tested indicating that flame propagation through unburnt mixture of CH4 and C8H18 hydrocarbon fuels is not chemically controlled but controlled by dint of turbulent diffusion.

Heat release term due to chemical reactions on right hand side of energy equation is of no importance for flame front shape and its displacement yielding the conclusion that aforementioned invariance is valid for broad range of hydrocarbon fuels.

5. References

[1] J.Danneman, K.Pielhop, M. Klaas, W. Schroeder(2010) „Cycle resolved multi planar flow measurements in a four valve combustion engine", Exp.Fluids, Research article, DOI 10.1007/s00348-010-0963-4

[2] Z. Jovanovic, S. Petrovic "The mutual interaction between squish and swirl in IC Engines", (1997) Mobility and Vehicle Mechanics 23, 3, 72-86

[3] K. Lee, C. Bae, K. Kang "The effects of tumble and swirl flows on flame propagation in a four-valve S.I.engine", Applied Thermal Engineering 27 (2007) 2122-2130

[4] G.J.Micklow, W. D. Gong "Intake and in cylinder flow field modeling of a four valve diesel engine" Proc.IMechE(2007) vol. 221, Journal of Automobile Engineering, 1425-1440

[5] B. Khaligi "Intake generated swirl and tumble motion in a 4.-valve engine with various intake configurations" SAE Paper 900059

[6] Z.Jovanovic, S. Petrovic, M. Tomic "The effect of combustion chamber geometry layout on combustion and emission" (2008) Thermal Science vol.12, No.1, pp. 7-24

[7] Z. Jovanovic, Z.Masonicic, M. Tomic „The vice-verse movement of the reverse tumble centre of rotation in a particular combustion chamber", MTM Machines Technologies Materials, Year II, issue 6-7, (2008) ISSN 1313-0226l, pp. 17-20

[8] Z. Masonicic, Z. Jovanovic "The effect of combustion chamber geometry layout variations onto fluid flow pattern", International Automotive Conference with Exhibition, SCIENCE AND MOTOR VEHICLES, NMV0774, Belgrade, 2007, ISBN 978-86-80941-31-8

[9] Z.Jovanovic "The role of tensor calculus in numerical modeling of combustion in IC engines" Computer Simulation in Fluid Flow, Heat and Mass Transfer and Combustion in Reciprocating Engines, Hemisphere Publishers (1989) 457-542, ISBN 0-89116-392-1

[10] CFD Solver, AVL FIRE 2009.1

[11] C.G. Speciale, S. Sarkar, T. B. Gatski „Modelling the pressure strain correlation of turbulence – an invariant dynamical system approach", pp.1-51, ICASE Report No. 90-5, 1990

[12] Z. Jovanovic, Z. Masonicic, Z. Živanovic, Ž. Šakota, Dj.Diligenski, M.Milovanovic, The effect of turbulence model variation on flame propagation in 4.-valve engines, trans & MOTAUTO '13, CD, Varna, jun 2013, ISSN 1310-3946

[13] K.Hanjalic, M.Popovac, M.Hadjiabdic „A robust near-wall elliptic relaxation eddy viscosity turbulence model for CFD", International Journal of Heat and Fluid Flow, 25(2004) 1047-1051

[14] P.A.Durbin „Near wall turbulence closure modeling without damping functions", Theor.Comput. Fluid Dynamics (1991) 3 1-13